High accuracy, wide range, rotation angle measurement by the use of two parallel interference patterns

Xiaoli Dai, Osami Sasaki, John E. Greivenkamp, and Takamasa Suzuki

Based on the idea of measuring small rotation angles with a parallel interference pattern (PIP), a method is developed to measure large rotation angles accurately. Two parallel PIP's that have different periods are used to measure a rotation angle of an object. The measurement made with a small-period PIP provides a high accuracy, and the measurement made with a large-period PIP provides a wide range. An accurate measurement for wide-range angles is made by combining the two measured values. The accuracy of the phase detection is determined by the periods of two PIP's. Rotation angles from approximately −30 to 30 arc min can be measured with an accuracy of 0.2 arc sec. Analytical results are supported by experimental results. © 1997 Optical Society of America

Key words: Wide range, high accuracy, rotation angles, interferometry.

1. Introduction

Several optical methods based on interferometry,[1-5] autocollimation,[6-7] the internal reflection effect,[8] and the moiré technique[9] have been proposed for measurements of angles. However, for most of these methods, it is difficult to achieve both high accuracy and wide range. For this problem to be solved, a method based on the idea of measuring small rotation angles by using a parallel interference pattern (PIP)[1] is developed to measure wide-range rotation angles accurately.

With the use of a single PIP, the measurement range is limited to a phase change of 2π because of ambiguity in the phase detection technique. This corresponds to measuring a shift of one fringe. The measurement range is proportional to the period of the PIP, and the measurement accuracy is inversely proportional to the period of the PIP. Thus it is impossible to get both high accuracy and wide range by using one PIP. Here we use two parallel PIP's that have different periods. A large rotation causes a phase change of the large-period PIP of less than 2π, and a measured value is obtained. This measured value eliminates phase ambiguities of 2π in a measured value obtained from the small-period PIP. The technique to combine the two measured values is the same as that used in two-wavelength interferometry.[10] The system measurement accuracy maintains the high accuracy that can be obtained with the small-period PIP, and the measurement range is as large as that obtained from the large-period PIP. Therefore, the system measurement range of a rotation angle is extended without sacrificing the high measurement accuracy.

In Section 2 a theoretical analysis shows how to combine the two measured values to obtain an accurate result for large rotation angles. In Section 3 we present an experimental setup in which we use two sinusoidal phase-modulating interferometers with feedback-control systems to eliminate the effects of mechanical vibrations. The phases of PIP's are detected with optical fibers. In Section 4 we describe how to determine the periods of two PIP's when the measurement accuracy of the phase depends on characteristics of the optical fibers. In Section 5 we show that the experimental results agree well with the theoretical analysis. By using the two PIP's with periods of 500 μm and 4.5 mm, we measure rotation angles from approximately −30 to 30 arc min with an accuracy of 0.2 arc sec.
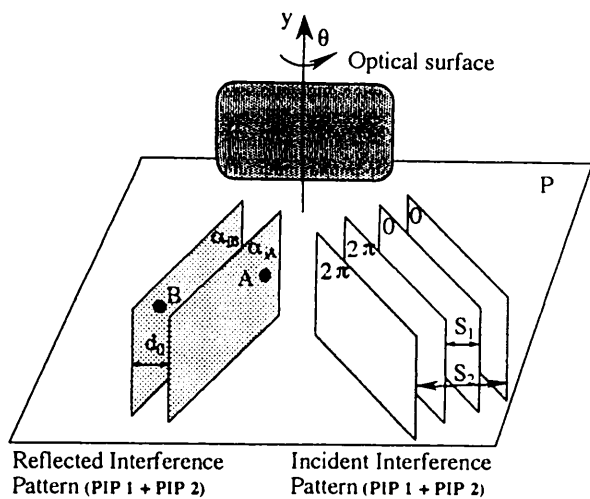
Fig. 1. PIP's of two different periods reflected by an optical surface.

Fig. 2. Fundamental configuration to measure a rotation angle.

2. Principle

Two PIP's that have different periods and are parallel with each other are shown in Fig. 1. The period of the PIP $i(i = 1, 2)$ is expressed as S_i. The value of S_2 is larger than the value of S_1 and

$$S_2 = mS_1, \qquad (1)$$

where $m > 1$. The phase difference between the two beams forming the PIP is called the phase of the PIP. We define a plane on which the phases of the PIP are constant as an equiphase plane (EPP). The object is an optical surface that rotates around the y axis and reflects the incident PIP's. We refer to a plane perpendicular to the y axis as plane P. The EPP's are perpendicular to plane P and are reflected by the optical surface. Phases of the reflected EPP's are detected at points A and B. The phases of the EPP's that contain points A and B are expressed as α_{iA} and α_{iB}, respectively, where α_{1A}, α_{1B} are the phases of PIP 1 and α_{2A}, α_{2B} are the phases of PIP 2.

The phase difference is expressed as

$$\alpha_{i0} = |\alpha_{iB} - \alpha_{iA}|, \qquad (2)$$

where $0 \le \alpha_{i0} \le 2\pi$. The distance d_0 is smaller than the period S_2 of PIP 2. We obtain two different expressions of d_0 by using PIP 1 and PIP 2, respectively. Because the value of α_{10} is within 2π for PIP 1 even if the d_0 is more than nS_1, we have

$$d_0 = nS_1 + \frac{\alpha_{10}}{2\pi}S_1, \qquad (3)$$

where n is a nonnegative integer. For PIP 2, we have

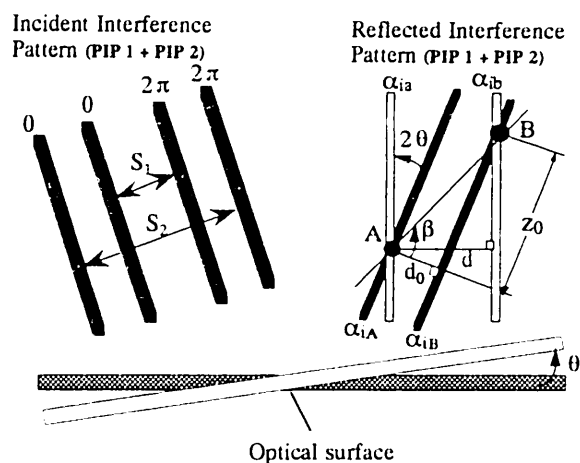$$d_0 = \frac{\alpha_{20}}{2\pi}S_2. \qquad (4)$$

From Eqs. (3) and (4), we have

$$\alpha_{20} = \frac{2\pi n + \alpha_{10}}{m}. \qquad (5)$$

Let us consider how the distance d_0 changes by rotation of the object. A top view of the arrangement in Fig. 1 is shown in Fig. 2. The line passing the phase detection points A and B is referred to as a detection line. The angle between the detection line and the line perpendicular to the reflected PIP is denoted by β. We have

$$\tan \beta = z_0/d_0, \qquad (6)$$

where z_0 is the distance of points A and B along the parallel interference fringes. Before a rotation of the mirror, the phases of the two EPP's that contain points A and B are expressed as α_{iA} and α_{iB}, respectively. When the optical surface rotates by an angle θ, the reflected PIP 1 and PIP 2 rotate by an angle 2θ. The distance d_0 changes to d. The phases detected at points A and B change to α_{ia} and α_{ib}, whose difference is expressed as

$$\alpha_i = |\alpha_{ib} - \alpha_{ia}|, \qquad (7)$$

where $0 \le \alpha_i \le 2\pi$. From the geometrical relationship between distances d_0 and d as shown in Fig. 2, we have

$$d = \frac{\cos(\beta - 2\theta)}{\cos \beta} d_0. \qquad (8)$$

By using approximations for trigonometric function, such as $\sin 2\theta \cong 2\theta$, $\cos 2\theta \cong 1$, when the angle θ is smaller than $5°$, Eq. (8) reduces to

$$\theta = (d - d_0)/2z_0. \qquad (9)$$

From Eq. (9), the value of θ is positive when $d > d_0$ and the value of θ is negative when $d < d_0$. So, we state that the rotation direction of the optical surface that is shown in Fig. 2 is positive and the opposite rotation direction is negative.

First let us consider an expression of the rotation angle θ by using PIP 1. The distance d is given by

$$d = n'S_1 + (\alpha_1/2\pi)S_1, \qquad (10)$$

where n' is a nonnegative integer. On substitution of Eqs. (3) and (10) into Eq. (9), the expression of θ is given by

$$\theta = NS_1/2z_0 + \theta_1, \qquad (11)$$

where $N = n' - n$ and

$$\theta_1 = (\alpha_1 - \alpha_{10})S_1/4\pi z_0. \qquad (12)$$

The measurement error of θ_1 caused by the random error in the measurement of α_{10} and α_1 is estimated with its standard deviation σ_{θ_1}, which is given by[1]

$$\sigma_{\theta_1} = S_1\sqrt{2}\,\sigma/4\pi z_0, \qquad (13)$$

where σ is the standard deviation of phase differences α_{10}, α_1. We see that the measurement accuracy of θ_1 is very high when S_1 is small. When $\alpha_{10} = \pi$, the symmetric measurement range for the positive and negative rotation angles is obtained. The absolute measurement range of θ_1 is given by[1]

$$\theta_{1\,\text{max}} = \frac{S_1}{2z_0}. \qquad (14)$$

The measurement range of θ_1 is very narrow when S_1 is small. From Eq. (14), Eq. (11) is rewritten as

$$\theta = N\theta_{1\,\text{max}} + \theta_1. \qquad (15)$$

If the value of N is accurately determined, the measurement accuracy of θ is equal to that of θ_1.

Second, let us discuss how to determine the value of N. In the condition of $d \le S_2$, we obtain a value for θ that is measured by using PIP 2; this is denoted by θ_2 as

$$\theta_2 = (\alpha_2 - \alpha_{20})S_2/4\pi z_0. \qquad (16)$$

Because the period S_2 of PIP 2 is m times as large as the period S_1 of PIP 1, the absolute measurement range increases, but the accuracy decreases. On substituting Eqs. (12) and (14) into the right-hand side of Eq. (15) and using Eq. (16) as the left-hand side of Eq. (15), the expression of N is obtained as

$$N = [(\alpha_2 - \alpha_{20})m - (\alpha_1 - \alpha_{10})]/2\pi. \qquad (17)$$

The measurement error of N caused by the random error in the measurement of α_{10}, α_1, α_{20}, and α_2 is estimated with its standard deviation σ_N. From Eq. (17), we have

$$\sigma_N = \sigma\sqrt{2(m^2 + 1)}/2\pi. \qquad (18)$$

The integer N is decided exactly when the condition of $3\sigma_N < 0.5$ is satisfied. This condition is equivalent to $3\sigma_{\theta_2} < \theta_{1\,\text{max}}$, that is, the accuracy of the measurement with a large-period PIP is less than the range of the measurement with the small-period PIP. The angle θ is obtained from Eq. (15) when values of θ_1
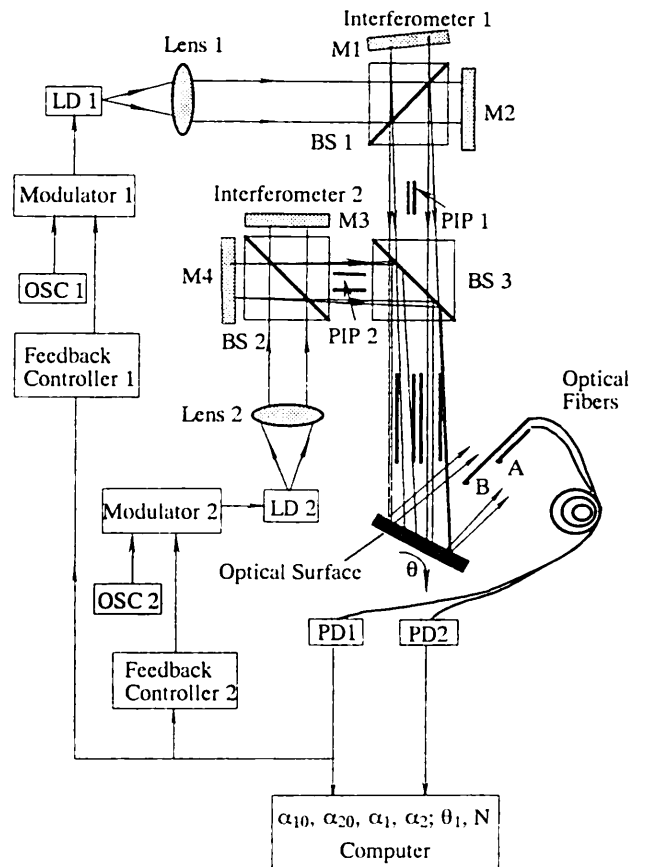

Fig. 3. Experimental setup; OSC, oscillator.

and N are measured by Eqs. (12) and (17), respectively. It is clear that the measurement accuracy of θ is equal to that of θ_1 after the integer N is accurately determined.

Next we have an interest in measurement ranges of N and θ in Eq. (15). From Eqs. (5) and (17), the measurement range of N is

$$-n \le N \le m - n - 1. \qquad (19)$$

The absolute measurement range of N is equal to $m - 1$, and the absolute measurement range of θ in Eq. (15) is $m\theta_{1\,\text{max}}$. Therefore, the measurement range is as wide as one obtained from the large-period PIP. In addition, we obtain $n = (m - 1)/2$ in the condition of $\alpha_{10} = \alpha_{20} = \pi$ from Eq. (5). Then the measurement range of N is from $-(m - 1)/2$ to $(m - 1)/2$, and the measurement range of θ in Eq. (15) is

$$-m\theta_{1\,\text{max}}/2 \le \theta \le m\theta_{1\,\text{max}}/2. \qquad (20)$$

Thus, for one to obtain the symmetric measurement range for positive and negative angles, the condition of $\alpha_{10} = \alpha_{20} = \pi$ is required. This condition is satisfied if $\alpha_{20} = \pi$ and $m = 2n + 1$.

3. Optical System

As shown in Fig. 3, two Twyman–Green type of interferometers are used to generate two different PIP's. The wavelength of laser diode LD i ($i = 1, 2$)

is 780 nm. The diameters of collimated beams are ~8 mm. In the interferometer $i(i = 1, 2)$, a PIP occurs when two collimated laser beams intersect with an angle γ_i. The fringes exist everywhere the two beams overlap. Because angle γ_i is small, the overlap length of the two laser beams or the length of the parallel interference pattern is long enough for our experiment. The PIP i is perpendicular to plane P, which is regarded as the plane of the figure. Beam splitter (BS) 3 is used to make the two PIP's overlap each other. The incident angle of the PIP's onto the optical surface is ~5°.

As shown in Fig. 3, when the optical surface is removed, the two beams from BS 1 separate at a position far from the optical surface and are observed as two spots on a plane perpendicular to plane P. When the distance from mirror M 1 to the observed spots is expressed as L_1 and the distance between the centers of two observed spots is expressed as H_1, the value of angle γ_1 is obtained by the ratio of H_1 to L_1. To obtain an enough accuracy for angle γ_1, a long distance L_1 of approximately a few meters is necessary. Angle γ_2 is also adjusted in the same manner. In contrast, the distance between the centers of two spots along a line perpendicular to plane P tells us how PIP i is perpendicular to plane P. When the four spots from BS 1 and BS 2 are on a line parallel to plane P, the two PIP's are exactly perpendicular to plane P. The center of the line connecting the two spots from BS 1 must be coincided with the center of the line connecting the two spots from BS 2 to obtain the two PIP's that are parallel to each other. In our experiment, $S_1 = 0.5$ mm and $S_2 = 4.5$ mm at $\gamma_1 = 5.36'$ and $\gamma_2 = 35.6''$, respectively.

Two fibers stuck together are used to detect the interference signals at two points A and B. The outsider diameters of the fibers are ~1 mm, and their core diameters are 50 μm. The optical fibers are placed parallel to plane P and along the propagation direction of reflected laser beams to receive the light at points A and B. The distances d_0 and z_0 between points A and B can easily be changed by moving the position of optical fibers. In our experiment, $d_0 = S_2/2$, and $z_0 = 120$ mm.

In the interferometers, the injection currents of the laser diodes are modulated with a sinusoidal signal to change the wavelength of the laser diodes, and sinusoidal phase-modulating interferometry is used. As a way to distinguish the two interference signals of interferometers 1 and 2, the modulation frequencies of the injection currents of two laser diodes are 8 and 1 kHz, respectively.[11] Two optical fibers are connected with two photodiodes (PD's) 1 and 2 to detect the interference signals. The interference signals are sent into a computer through an analog-to-digital converter. By the use of the technique of sinusoidal phase-modulating interferometry, the phases of the interference signals are detected. Thus we obtain two phase differences α_{10} and α_{20} for PIP 1 and PIP 2, respectively. After the optical surface rotates, in the same way we also obtain two phase differences α_1 and α_2 for PIP P_1 and PIP P_2, respectively. There-
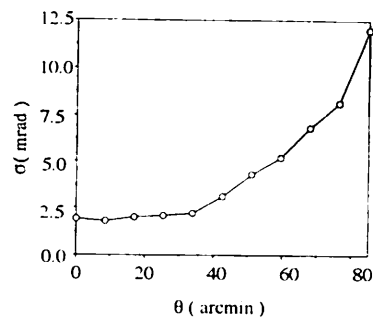

Fig. 4. Relationship between the rotation angle and the error in phase detection.

fore, with α_{10}, α_{20}, α_1, and α_2, the values of θ_1 and N are obtained by Eqs. (12) and (17). Feedback controllers 1 and 2 are used in interferometers 1 and 2, respectively, to eliminate the fluctuations of phases that are caused from mechanical vibrations.[12] The random errors in the measurement of the phase differences are greatly decreased. A standard deviation σ of phase differences α_{10}, α_{20}, α_1, and α_2 can be decreased from 0.1 rad to 2 mrad by using the feedback-control systems.

4. Determination of Periods S_1 and S_2

The core diameters of graded-index optical fibers were 50 μm. For the phases of the PIP to be detected exactly, it is desirable that the value of S_1 is approximately ten times the core diameter of the optical fiber. Period S_1 was 500 μm. We obtained an accuracy of 2 mrad for the phase detection when the direction of the light incident upon the optical fiber was almost perpendicular to the face of the optical fiber and the center of the light was on the center of the face of the fiber. The accuracy is not kept while the rotation angle becomes large. Because the center of the light moves off the center of the face of the fiber at a large rotation angle, the intensity of the light received with the optical fiber decreases. A weak received light increases the standard deviation σ of the phase differences α_{10}, α_{20}, α_1, and α_2. To investigate the property of the optical fibers, we did the experiment whose results are shown in Fig. 4. The measured object was a mirror, which was rotated at intervals of 8.5 arc sec. Phase α_1 was detected ten times within 5 min every time the mirror rotated by one interval. We obtained the standard deviation σ of the random errors in the phase detection. We found that the value of σ became larger as the rotation angle θ became larger. The value of σ was beyond 2 mrad when the rotation angle θ was larger than ~40 arcmin. To obtain a high measurement accuracy, we keep an accuracy of 2 mrad for phase detection. Then we limit the maximum rotation angle to 40 arc min, that is, $\theta_{max} = 40$ arc min. When $\alpha_{20} = \pi$, the symmetric measurement range for the positive and negative rotation angle θ_2 is $S_2/4z_0$. This range must be equal to or a little smaller than θ_{max} to keep the accuracy of 2 mrad in this range. Thus we have $S_2 \leq 4z_0\theta_{max}$. When $\alpha_{20} = \pi, z_0 = 120$
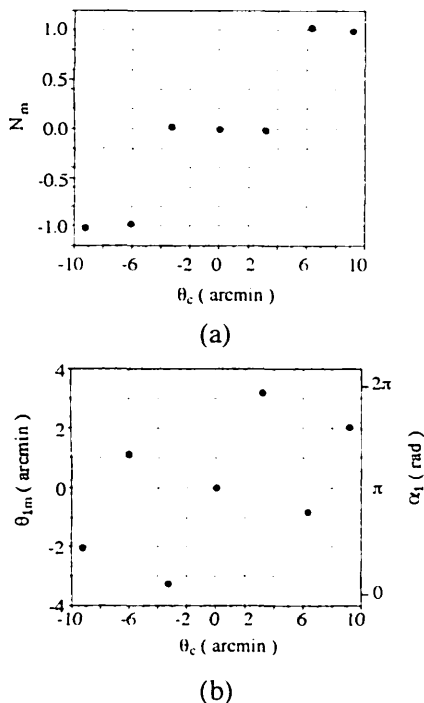
(a)

(b)

Fig. 5. Measurement of rotation angles by our method and an autocollimator: (a) measurement results of N_m, (b) measurement results of θ_{1m}.

Table 1. Measurement Results of Small Rotation Angles

θ_c	N_m	N	θ_{1m}	θ_m	ε
$-9'12.0''$	-1.01	-1	$-2'2.5''$	$-9'12.2''$	$0.2''$
$-6'3.5''$	-0.99	-1	$1'6.4''$	$-6'3.3''$	$-0.2''$
$-3'16.5''$	0.01	0	$-3'16.3''$	$-3'16.3''$	$-0.2''$
$0.5''$	-0.01	0	$0.3''$	$0.3''$	$0.2''$
$3'10.5''$	0.01	0	$3'10.3''$	$3'10.3''$	$0.2''$
$6'20.0''$	1.01	1	$-49.5''$	$6'20.2''$	$-0.2''$
$9'11.3''$	0.99	1	$2'1.4''$	$9'11.1''$	$0.2''$

mm, and $\theta_{max} = 40$ arc min, we have $S_2 < 5.59$ mm. In our experiment, the value of m was taken to be an odd number to obtain a symmetric measurement range for positive and negative angles. The value of m was 9 and period S_2 was 4.5 mm. From Eq. (18), we had $3\sigma_N \approx 0.012$ for $\sigma \approx 2$ mrad and $m = 9$. The condition of $3\sigma_N < 0.5$ was satisfied.

5. Measurements

We did experiments with the experimental setup shown in Fig. 3. Because the value of m is odd and $\alpha_{20} = \pi$, $\alpha_{10} = \pi$ and $n = 4$. As a way to examine the principle of our method, the rotation angle θ was measured by our method and with an autocollimator. As shown in Fig. 5, the rotation angle θ was given at intervals of ~ 3 arc min from approximately -9 to 9 arc min by the autocollimator. The values measured with the autocollimator are expressed as θ_c. At each value of θ_c, we detected the values of α_1 and α_2. From Eqs. (12) and (17), we obtained the values of θ_1 and N, respectively. Their measured values are expressed as N_m and θ_{1m} and are shown in Figs. 5(a) and 5(b), respectively. Figure 5(a) shows that the value of N_m is not an integer and is almost 1, 0, and -1. The differences of N_m from 1, 0, and -1 are ~ 0.01, which is caused from the error σ_N. Although the experimental value of $\sigma_N \approx 0.01$ was a little different from the theoretical value of $\sigma_N \approx 0.004$ obtained from Eq. (18), the condition of $3\sigma_N < 0.5$ was satisfied in the experiments. From the value of N_m, we obtained the value of N as shown in Table 1. The measurement results in Fig. 5(b) show that the value of θ_{1m} changes from approximately -3 arcmin to 3

arcmin. The measurement range of θ_1 is between $-\theta_{1\,max}/2$ and $\theta_{1\,max}/2$ in the condition of $\alpha_{10} = \pi$, where $\theta_{1\,max} = 7'9.7''$. We obtained the measured values of $\theta_m = \theta_{1m} + \theta_{1\,max}N$ and an error of $\varepsilon = \theta_c - \theta_m$ as shown in Table 1. The results show that the standard deviation σ_{θ_1} of the random error caused from the measurement of θ_{1m} is approximately ± 0.2 arc sec. The theoretical value of σ_{θ_1} given by Eq. (13) is 0.2 arc sec at $\sigma = 2$ mrad.

Next we tried to make a measurement over the whole range. The object was rotated at intervals of 10.2 arc min from approximately -40 to 40 arc min. The rotation angles were measured by our method. The measurement results of N_m and α_2 at each rotation are shown in Fig. 6. We observed that the value of α_2 jumps over 2π for large rotation angles. This observation indicates that the measurement range of N is from -4 to 4 and that the measurement range of rotation angle θ obtained from Eq. (16) is from ~ 32 arcmin to 32 arcmin. The theoretical values given by relations (19) and (20) are $-4 \leq N \leq 4$ and $-32'13''$ $\leq \theta \leq 32'13''$, respectively. Analytical results described in Section 2 have been supported by the experimental results.

6. Conclusions

Based on the idea of measuring small rotation angles with a PIP, a method of measuring a large rotation angle has been presented. Because of the phase ambiguities in the phase detection technique, the measurement range given by the use of a small-period PIP is small. To widen the measurement range, we use a large-period PIP together with the small-period PIP to eliminate a phase ambiguity of $2\pi N$. By a combination of the two values measured with the two PIP's, the integer N is accurately determined if the
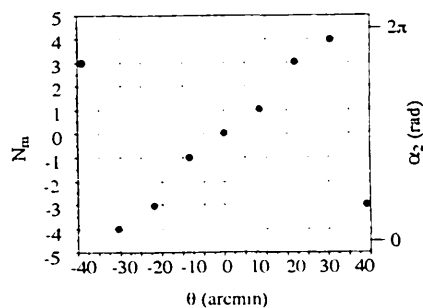

Fig. 6. Measurement results of N_m for wide-range rotation angles.

standard deviation σ_N of N satisfies the condition $3\sigma_N < 0.5$. This condition means that the measurement error from the large-period PIP is smaller than the measurement range from the small-period PIP. When the ratio of two periods or the standard deviation σ of the random error in the phase detection is small, this condition is easily satisfied. With this, the measurement accuracy is as high as one obtained from the small-period PIP, and the measurement range is as wide as one obtained from the large-period PIP. In the experiments, the accuracy of the phase detection for rotation angles depends greatly on the characteristics of the optical fibers. For a large rotation angle, the accuracy of the phase detection becomes low because the light received with the optical fibers becomes weak. A maximum rotation angle is limited so that the accuracy of the phase detection is higher than a specified value σ_s. This condition determines the large period S_2 of the PIP. The small period S_1 of the PIP is determined by the core diameter of the optical fiber. When $S_1 = 500$ μm, $S_2 = 4.5$ mm, and $\sigma_s = 2$ mrad, rotation angles were measured with a high accuracy of 0.2 arcsec in the range from approximately -30 arcmin to 30 arcmin.

References

1. X. Dai, O. Sasaki, J. E. Greivenkamp, and T. Suzuki, "Measurement of small rotation angles by using a parallel interference pattern," Appl. Opt. **34**, 6380–6388 (1995).
2. J. G. Marzolf, "Angle measuring interferometer," Rev. Sci. Instrum. **35**, 1212–1215 (1964).
3. G. D. Chapman, "Interferometric angular measurement," Appl. Opt. **13**, 1646–1651 (1974).
4. T. Takano and S. Yonehara, "Basic investigations on an angle measurement system using a laser," IEEE Trans. Aerosp. Electron. Syst. **26**, 657–662 (1990).
5. P. Shi and E. Stijns, "New optical method for measuring small-angle rotations," Appl. Opt. **27**, 4342–4344 (1988).
6. P. R. Yoder, Jr., E. R. Schlesinger, and J. L. Chickvary, "Active annular-beam laser auto-collimator system," Appl. Opt. **14**, 1890–1895 (1975).
7. F. J. Schuda, "High-precision, wide-range, dual-axis, angle monitoring system," Rev. Sci. Instrum. **54**, 1648–1652 (1983).
8. P. S. Huang, S. Kiyono, and O. Kamada, "Angle measurement based on the internal-reflection effect: a new method," Appl. Opt. **31**, 6047–6055 (1992).
9. B. P. Singh, K. Varadan, and V. T. Chitnis, "Measurement of small angular displacement by a modified moiré technique," Opt. Eng. **31**, 2665–2667 (1992).
10. Y. Y. Cheng and J. C. Wyant, "Two-wavelength phase shifting interferometry," Appl. Opt. **23**, 4539–4541 (1984).
11. O. Sasaki, H. Sasazaki, and T. Suzuki, "Two-wavelength sinusoidal phase-modulating laser-diode interferometer insensitive to external disturbances," Appl. Opt. **30**, 4040–4045 (1991).
12. O. Sasaki, K. Takahashi, and T. Suzuki, "Sinusoidal phase modulating laser diode interferometer with a feedback control system to eliminate external disturbance," Opt. Eng. **29**, 1511–1515 (1990).